Atsushi Fujimori, et. al. International Journal of Engineering Research and Applications
www.ijera.com
ISSN: 2248-9622, Vol. 10, Issue 7, (Series-V) July 2020, pp. 48-59

RESEARCH ARTICLE OPEN ACCESS

Formation Control of Multi-Sonar Equipped Mobile Robots and Large Obstacle Avoidance

Atsushi Fujimori[*1], Atsushi Hosono[*2], Shinji Kuratani[*3], Shinsuke Oh-hara[*4]
**1 (Department of Mechanical Engineering, University of Yamanashi, Japan*
**2 (Department of Mechanical Engineering, University of Yamanashi, Japan*
**3 (Department of Mechanical Engineering, University of Yamanashi, Japan*
**4 (Department of Mechanical Engineering, University of Yamanashi, Japan*

ABSTRACT
This paper presents a formation control of multi-sonar equipped mobile robots with large obstacle avoidance. Based on our previous navigation techniques, new strategies for avoiding large sized obstacles and reinforce modules are newly introduced. The effectiveness of the proposed techniques is demonstrated in the experiments using three real mobile robots with three types of obstacles; longitudinal-ellipsoid, lateral-ellipsoid and wall obstacles.
Keywords **-** Formation control, leader-follower method, obstacle avoidance, sonar assignment

---

Date of Submission: 06-07-2020 Date of Acceptance: 21-07-2020

I. INTRODUCTION

Formation control of multiple mobile robots has attracted much attention for the last decade. As this background, the formation is effective in traffic systems of automobile and aircraft and may be needed for cooperation between multiple robotic systems. On formation control of mobile robots, the following three approaches; leader-follower graphs [1], [2], reactive behaviors [3], [4] and virtual structure [5] have been studied from several points of view. On the other hand, the sensor used on mobile robot influences performance of the formation control that can be realized. Formation control of multi-sonar equipped mobile robots has been examined by the leader-follower technique [6] – [9]. Follower robots detect the leader robot by using multiple sonars and are then controlled to keep a relative position which is specified in advance. Fujimori et al. [6], [8] proposed a distributed control law, called self-made input (SMI), which did not need information exchange between a leader robot and follower robots and estimated the states of the leader robot. Furthermore, it was shown in [7], [9] that formation control with obstacle avoidance was realized by using multiple sonars for leader tracking and obstacle detection adaptively. In the experiments performed in the previous studies [7], [9], the avoidance action was small because the obstacle there was almost the same size as the mobile robots. For large sized obstacles, however, the formation control was failed; that is, the follower robots did not avoid obstacles completely and/or lost the leader robot to be tracked.

This paper proposes improved navigation techniques for formation control with large obstacle avoidance. The size of obstacle considered in this paper is larger than three times of the mobile robots. Based on the techniques in [9], the following novel modules are proposed. When the obstacle avoidance is not finished within a specified time, the follower robot judges that the size of the obstacle encountered is large. The follower robot then decides to change the formation shape for accomplishing the obstacle avoidance. After avoiding the obstacle, the formation shape is returned to the original one. As additional modules for supporting the sonar assignment and the leader estimation, new modules, called *Sonar Prediction* and *Move Prediction*, are newly introduced in the proposed navigation algorithm. The strategy mentioned above was originally proposed in [10], but some drawbacks which should be improved were included. This paper therefore gives modification for them and presents the experimental results of formation control under more complicated environments to verify the effectiveness of the proposed techniques.

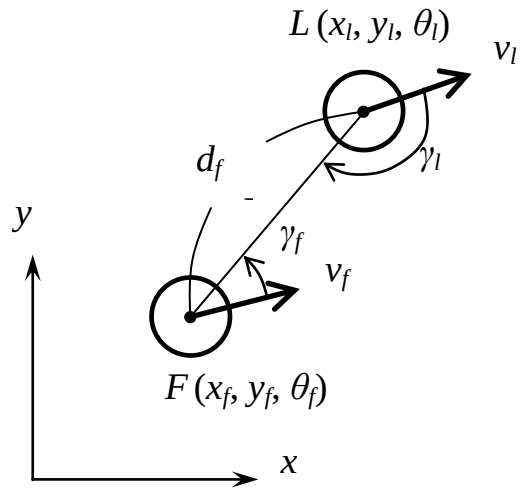

Figure 1: A status of leader-follower formation control by two mobile robots.

II. FORMATION CONTROL OF SONAR EQUIPPED MOBILE ROBOTS WITH OBSTACLE AVOIDANCE

This section presents the statements of problem for formation control of multi-sonar equipped mobile robots with obstacle avoidance considered in this paper. The statements of formation control of the mobile robots are described. The mobile robots used in the experiments are shown. The navigation algorithm in the previous study [9] is shown and the modules in the algorithm are briefly explained.

A. Formation Control by Leader-Follower Method

This subsection shows the notations for mobile robots considered in the formation control and the control objective by the leader-follower method. The position of the mobile robot in the two-dimensional plane is denoted by the Cartesian coordinates (x,y). Its directional angle from the positive x-axis is denoted by $\theta(t)$. The control commands of the mobile robot are the linear and the angular velocities $v(t)$ and $\omega(t)$. The equation of kinematics of the mobile robot is then given by

$$\begin{cases} \dot{x}(t) = v(t)\cos\theta(t) \\ \dot{y}(t) = v(t)\sin\theta(t) \\ \dot{\theta}(t) = \omega(t) \end{cases} \quad (1)$$

The magnitudes of the control commands are constrained as

$$|v(t)| \leq v_{\max}, \quad |\omega(t)| \leq \omega_{\max} \quad (2)$$

where $v_{\max}$ and $\omega_{\max}$ are the maximum values of $v(t)$ and $\omega(t)$, respectively.

A status of the leader-follower formation control by two mobile robots is depicted in Fig. 1, where the leader robot is denoted as L and the follower F. Hereafter, the subscript l and f in the notations mean *leader* and *follower*, respectively. The equations of L and F are expressed as Eq. (1) using their own variables. The relative distance between the leader and the follower robots is denoted as d_l $(=d_f)$ and the relative angles are denoted as γ_l and γ_f, respectively.

In the leader-follower method, d_f and γ_f are controlled to track their references d_f^{rel} and γ_f^{rel} with the nominal linear velocity, denoted v_0. Furthermore, if the mobile robots encounter an obstacle during formation control from a start to a goal, the mobile robots must avoid the collision with the obstacle. Without loss of generality, it is assumed that the start and the goal of the leader robot are located at the Cartesian coordinates of the origin and (x_g,y_g), respectively.

Since the control law which had been obtained by the dynamic inversion included the states and the control commands of both the leader and the follower robots [1], [11], some kinds of communication mean had been necessary between the leader and the follower robots to implement the control method on the systems. Fujimori et al. [6], [8] proposed a distributed follower control law, called self-made input (SMI). Estimating the states of the leader robot and supposing the behaviors of the mobile robots under formation control, the control law was constructed with only the states and the control commands of the follower robot. The SMI therefore does not need any communication means. The SMI is adopted for the control method of the formation control in this study.

B. Mobile Robots

Figure 2 shows photos of mobile robots [12] – [14] which are used for formation control in this study. The left and the middle photos show Pioneer-1 and the right photo shows Pioneer-3. The diameter of the robots is about 450 [mm]. They are driven by two reversible motors which include optical encoders for position sensing. Pioneer-1 has seven ultrasonic sonars, while Pioneer-3 has eight sonars. They are attached on the side of the body. Table 1 shows the attached angles of the sonars from the forward direction of the robot coordinates.

Table 1: Multiple sonars in Pioneer-1 and -3.

Sonar no.	φ_i [deg]	
i	Pioneer-1	Pioneer-3
0	90	90
1	30	50
2	15	30
3	0	10
4	-15	-10
5	-30	-30
6	-90	-50
7	-	-90

Figure 2: Pioneer-1 and -3.

As for the leader robot during the formation control, the use of the multiple sonars is only to find obstacles which must be avoided. On the other hand, as for the follower robot, it is not only to find the obstacles, but also detect the leader robot which is to be tracked. To do this, the follower robots must obtain the relative distance d_f and the relative angle γ_f to the leader robot. The use of the multiple sonars for the obstacle avoidance will be described in the next subsection. The rest of this subsection presents the calculation of d_f and γ_f from the outputs of the multiple sonars. Since an ultrasonic sonar, in general, has the directivity and the finiteness for sensing, the sonar outputs the distance signal in the specified range. Letting the output and the attached angle of the i-th sonar be denoted as s_i and φ_i, respectively, d_f and γ_f are calculated by

$$d_f = \frac{\sum_{i\in\mathrm{F}} w_i s_i}{\sum_{i\in\mathrm{F}} w_i} \tag{3}$$

$$\gamma_f = \frac{\sum_{i\in\mathrm{F}} w_i \varphi_i}{\sum_{i\in\mathrm{F}} w_i} \tag{4}$$

where w_i is the weighting coefficient of the i-th sonar and Φ is the set of sonars tracking leader. That is, d_f and γ_f are obtained by averaging the outputs of the fired sonars with the weighting. The details are given in [9].

C. Reactive Obstacle Avoidance

When the mobile robot encounters an obstacle which must be avoided, a reactive avoidance behavior is decided by using the outputs of the multiple sonars. This subsection presents the brief of the process in [7]. According to the fired sonars which find an obstacle in the specified range, the encountered aspect is classified into the following eight categories; *Front, Left, Right, Front-Left, Front-Right, Left-Front-Right, Left-Right* and *Back*. These are called the sub-modes in the collision avoidance. Then, the mobile robot avoids the obstacle by the control commands which are given for each sub-mode in advance.

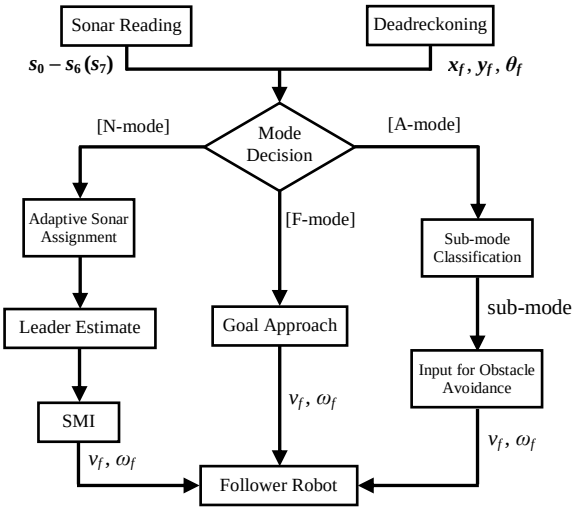

Figure 3: Navigation algorithm in [9].

D. Navigation Algorithm in [9]

Figure 3 shows the navigation algorithm which is constructed in [9]. Using the outputs of sonars $s_0 - s_6$ (s_7) obtained from *Sonar Reading* and the deadreckoning information x_f, y_f and θ_f, obtained from *Deadreckoning*, one of three modes is selected at *Mode Decision*, where N-mode indicates the formation control, A-mode indicates the obstacle avoidance and F-mode indicates the approach to goal.

In N-mode, multiple sonars are adaptively assigned for detecting the leader robot or obstacles at *Adaptive Sonar Assignment*. The position of the leader robot is estimated by using d_f and γ_f at *Leader Estimate*. The control commands v_f and ω_f for formation control are given at *SMI*.

In A-mode, the sub-mode is first decided at *Sub-mode Classificatio*n. The control commands for obstacle avoidance are given at *Input for Obstacle Avoidance*.

In F-mode, the control commands are given to make the mobile robot reach the goal.

III. CONTROL STRATEGY FOR LARGE OBSTACLE AVOIDANCE

This section proposes novel techniques for formation control with large obstacle avoidance. First, problems included in the previous navigation algorithm [9] are pointed out. The modified algorithm including novel modules is then proposed.

A. Problems in Previous Algorithm

This subsection explains problems when the previous algorithm is applied to formation control with large obstacle avoidance. Figures 4 (a), (b) and (c) depict aspects that three mobile robots avoid a large sized obstacle toward the left-hand side with keeping a triangle formation shape, denote *Triangle* hereafter, where L is the leader robot and F_1 and F_2 are the follower robots. In Fig. 4(a), L almost finishes avoiding the obstacle and F_1 begins to avoid the obstacle. As shown in Fig. 4(b), when F_1 finds a free space between F_2 and the obstacle, the obstacle avoidance of F_1 is succeeded with keeping the formation as drawing the trace by the gray dashed-line. However, in the case of Fig. 4(c); that is, if F_1 did not find an enough free space in the front, then F_1 does not avoid the obstacle or misses the leader L; that is, the formation control is failed. As another failed case, Fig. 4(d) shows an aspect that F_1 is not able to detect the leader robot after avoiding the obstacle and returning to the original formation shape. This case is happened that the sonars for the leader robot tracking are not suitably assigned or the position of the leader robot is not properly estimated.

Since the obstacle avoidance presented in the previous study [9] was a sort of small perturbation on formation control, the obstacle avoidance was accomplished with keeping the formation. For large sized obstacles, explained in Fig. 4 so far, additional techniques are needed to overcome those problems.

B. Proposed Navigation Algorithm

This subsection proposes a modified navigation algorithm shown in Fig. 5. The modules presented in the previous algorithm in Fig. 3 are also included in this algorithm. Where *Obstacle Check* and N-f-mode in Fig. 5 are the same as those of *Mode Decision* and N-mode in Fig. 3, respectively. The main modifications of the proposed algorithm are given as follows. (i) Two sub-modes, called N-r-mode and N-s-mode, are set in N-mode newly and are selected at *Nav Select*. (ii) The modules related to the change of formation shape are inserted at the beginning of A-mode. (iii) *Sonar Prediction* and *Move Prediction* are added to reinforce the tasks of *Adaptive Sonar Assignment* and *Leader Estimate*, respectively. The dashed-line arrows mean exchange of the information between the modules. The rest of this subsection explains the new modes and the new modules in the discrete-time representation, where t_k means the time at the k-th sampling and T_s is the constant sampling time; that is, $t_k = kT_s$.

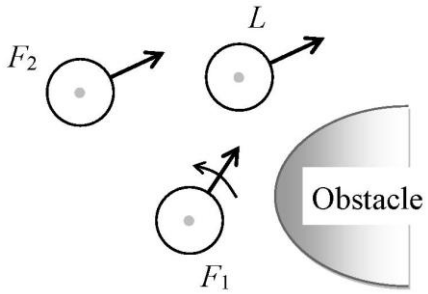

(a) At beginning of obstacle avoidance.

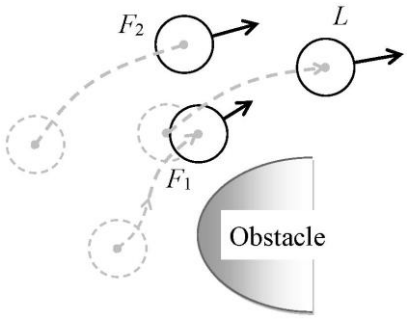

(b) A case where a free space is found between F_2 and obstacle.

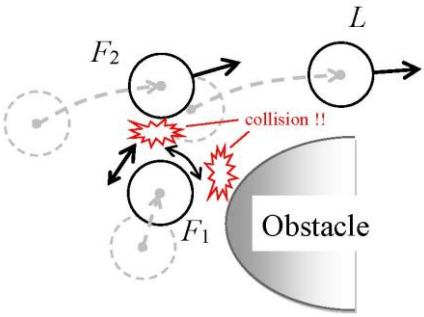

(c) Collision occurs with F_2 and obstacle.

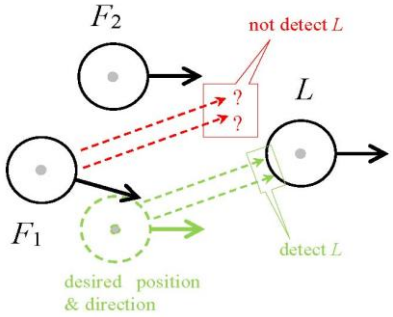

(d) F_1 does not detect L in N-mode after avoiding obstacle.

Figure 4: The situation that three mobile robots often meet during formation control in previous navigation algorithm [9].

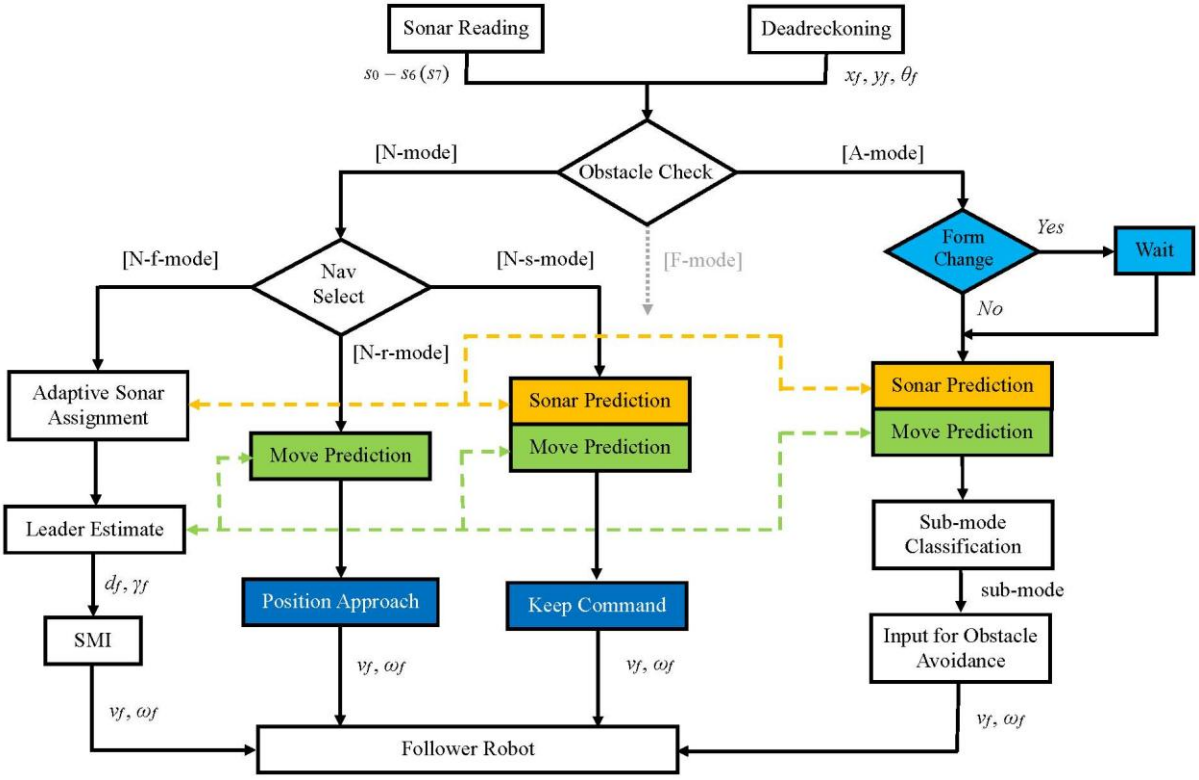

Figure 5: Proposed navigation algorithm.

(1) N-s-mode If the follower robot has not sufficiently avoided the obstacle in A-mode, the robot becomes unstable movement to repeat A-mode and N-mode frequently. To prevent this behavior, the previous control commands are maintained for a while after the mode was changed from A-mode to N-mode. It is managed at *Keep Command*.

(2) Form Change and Wait It may be always difficult for multiple mobile robots to avoid a large sized obstacle with keeping a formation shape although it depends on the shape of formation. In this situation, the shape should be changed to avoid the obstacle surely. This judgment is done at *Form Change* when N-s- and A-modes are repeated. In the concrete, the referenced relative distance $d_f^{\,rel}$ and the referenced relative angle $\gamma_f^{\,rel}$ for the new shape are re-defined.

As another technique, *Wait* module is inserted at the beginning of *Form Change* to avoid the collision with other follower robots and obtain an sufficient free space between them. After the follower robot waited for a while, it follows the new leader robot in the new formation shape.

(3) Sonar Prediction Sonars for the leader robot tracking are decided at *Adaptive Sonar Assignment* in N-f-mode. Since the direction of the follower robot is varied by the avoidance behaviors in A-mode, the sonars for the leader robot tracking may be not suitable after the mode returns from A-mode to N-mode. The proposed navigation algorithm introduces *Sonar Prediction* to correct the sonars which track the leader robot in A-mode and N-s-mode. Let us consider the case that the mode is changed from N-f-mode to A-mode or N-s-mode at $t=t_{ks}$. Letting $n_l(t_k)$ and $n_u(t_k)$ be respectively the lower and the upper number of sonars for the leader robot tracking, the following notations are defined for $k \geq k_s$.

$$\Delta n(t_k) \equiv n_u(t_k) - n_l(t_k) \tag{5}$$

$$\Delta\theta(t_k) \equiv \theta_f(t_k) - \theta_f(t_{ks-1}) \tag{6}$$

$\Delta n(t_k)$ is the difference of the number. $\Delta\theta(t_k)$ means the deviation of directional angle from the last N-f-mode. Then, $n_l(t_k)$ and $n_u(t_k)$ are shifted by comparing $\Delta\theta(t_k)$ to the attached angle of sonar φ_i. The algorithm for Pioneer-1 is given as follows.

if $(\Delta\theta(t_k) \geq \varphi_2)$ & $(\Delta\theta(t_k) < \varphi_1)$,
  then $n_u(t_k) \leftarrow n_u(t_k) + 1$
else if $(\Delta\theta(t_k) \geq \varphi_1)$ & $(\Delta\theta(t_k) < \varphi_0)$,
  then $n_u(t_k) \leftarrow n_u(t_k) + 2$
else if $(\Delta\theta(t_k) \geq \varphi_0)$,
  then $n_u(t_k) \leftarrow n_u(t_k) + 3$
if $(n_u(t_k) > 5)$, **then** $n_u(t_k) \leftarrow 5$
$n_i(t_k) = n_u(t_k) - \Delta n(t_k)$

if $(\Delta\theta(t_k) \le \varphi_4)$ & $(\Delta\theta(t_k) > \varphi_5)$,
then $n_l(t_k) \leftarrow n_l(t_k) - 1$
else if $(\Delta\theta(t_k) \le \varphi_5)$ & $(\Delta\theta(t_k) > \varphi_6)$,
then $n_l(t_k) \leftarrow n_l(t_k) - 2$
else if $(\Delta\theta(t_k) < \varphi_6)$,
then $n_l(t_k) \leftarrow n_l(t_k) - 3$
if $(n_l(t_k) < 1)$, **then** $n_l(t_k) \leftarrow 1$
$n_u(t_k) = n_l(t_k) + \Delta n(t_k)$

(4) Move Prediction At *Leader Estimate* in N-f-mode, d_f^{rel} and γ_f^{rel} are calculated by Eqs. (3) and (4), respectively, and the position of the leader robot is estimated. It is also useful in other modes to catch the position of the leader robot. The proposed navigation algorithm introduces *Move Prediction* to predict the position of the leader robot in the A-mode, N-s-mode and N-r-mode. $\hat{x}_l$, $\hat{y}_l$ and $\hat{\theta}_l$ are the estimated states of the leader robot. Let us consider the case that the mode is changed from N-f-mode to A-mode, N-s-mode or N-r-mode at $t=t_{km}$. To predict the position of the leader robot, it is assumed that the leader robot moves toward the goal with the normal linear velocity v_0 and the directional angle fixed at $\hat{\theta}_l(t_{km-1})$. Then, the positional coordinates of the leader robot $(\hat{x}_l(t_k), \hat{y}_l(t_k))$ for $k \ge k_m$ are predicted as

$$\begin{cases} \hat{x}_l(t_k) = \hat{x}_l(t_k) + v_0 T_s \cos\hat{\theta}_l(t_{km-1}) \\ \hat{y}_l(t_k) = \hat{y}_l(t_k) + v_0 T_s \sin\hat{\theta}_l(t_{km-1}) \end{cases} \quad (7)$$

Since the mode at $t=t_{km-1}$ was N-f-mode, the initial states $\hat{x}_l(t_{km-1})$, $\hat{y}_l(t_{km-1})$ and $\hat{\theta}_l(t_{km-1})$ are given by the estimated position at *Leader Estimate*.

(5) N-r-mode N-r-mode is introduced to re-construct the original formation shape after the follower robot finishes avoiding the obstacle completely. To do this, a target position is first set and the follower robot is then navigated to the target point. These are carried out in *Position Approach*. A concrete processing is explained by a situation that three mobile robots originally construct *Triangle*, where the leader robot is denoted as *L* and the two follower robots are denoted as F_1 and F_2. When F_1 encountered an obstacle, the shape of F_1 was changed to a line formation shape, denoted *Line*, by *Form Change*. After avoiding the obstacle completely, F_1 should be returned to construct the original formation shape *Triangle*. Then, let us consider the case that the mode of F_1 is changed to N-r-mode at $t=t_{kr}$. A target point, denoted *P* $(x_p(t_{kr}), y_p(t_{kr}))$, is defined as

$$\begin{cases} x_p(t_{kr}) = x_{f1}(t_{kr}) + \sqrt{2} d_{f1}(t_{kr}) \cos(\theta_{f1}(t_{kr}) - \frac{\pi}{4}) \\ y_p(t_{kr}) = y_{f1}(t_{kr}) + \sqrt{2} d_{f1}(t_{kr}) \sin(\theta_{f1}(t_{kr}) - \frac{\pi}{4}) \end{cases} \quad (8)$$

where $x_{f1}(t_{kr})$, $y_{f1}(t_{kr})$ and $\theta_{f1}(t_{kr})$ are the states of F_1 at $t=t_{kr}$. $d_{f1}(t_{kr})$ is the relative distance when F_1 followed F_2 in the shape of *Line*. Equation (8) is given by making (F_1, F_2, *P*) a right-angled isosceles triangle. The control commands of F_1 for $k \ge k_r$ are then given by

$$v_{f1}(t_k) = v_{\max} \quad (9)$$

$$\omega_{f1}(t_k) = K_p\{\gamma_p(t_k) - \theta_{f1}(t_k)\} \quad (10)$$

where K_p is a positive gain. $\gamma_p(t_k)$ is the relative angle for F_1; that is,

$$\gamma(t_k) \equiv \tan^{-1}\frac{y_p(t_k) - y_{f1}(t_k)}{x_p(t_k) - x_{f1}(t_k)}. \quad (11)$$

The target point *P* has to be updated with respect to time. By supposing that *L* moves toward its goal with the normal linear velocity v_0, the positional coordinates of the target point $(x_p(t_{kr}), y_p(t_{kr}))$ for $k \ge k_r$ are updated as

$$\begin{cases} x_p(t_{k+1}) = x_p(t_k) + v_0 T_s \cos\theta_p(t_{kr}) \\ y_p(t_{k+1}) = y_p(t_k) + v_0 T_s \sin\theta_p(t_{kr}) \end{cases} \quad (12)$$

where

$$\theta_p(t_{kr}) \equiv \tan^{-1}\frac{y_g - y_p(t_k)}{x_g - x_p(t_{kr})}. \quad (13)$$

(x_g, y_g) are the positional coordinates of the goal for *L*. It is thus possible that F_1 asymptotically return the original position of *Triangle* by Eqs. (9) – (13).

Furthermore, since the leader robot of F_1 after re-formation is *L*, it is necessary to modify the estimated position of the leader robot. $(\hat{x}_l(t_{kr-1}), \hat{y}_l(t_{kr-1}))$ are the estimated positional coordinates of F_2 because F_1 followed F_2 in the shape of *Line* for $t < t_{kr}$. The estimated positional coordinates of *L* are then given by

$$\begin{cases} \hat{x}_l(t_{kr}) = \hat{x}_l(t_{kr-1}) + d_{f1}^{ref}\cos(\theta_p(t_{kr}) + \gamma_{f1}^{ref}) \\ \hat{y}_l(t_{kr}) = \hat{y}_l(t_{kr-1}) + d_{f1}^{ref}\cos(\theta_p(t_{kr}) + \gamma_{f1}^{ref}) \end{cases} \quad (14)$$

where d_{f1}^{rel} and γ_{f1}^{rel} are the references for tracking *L*. The mode of F_1 is changed from N-r-mode to N-f-mode after F_1 reached near *P*. If F_1 catch *L* again, the re-formation is completed.

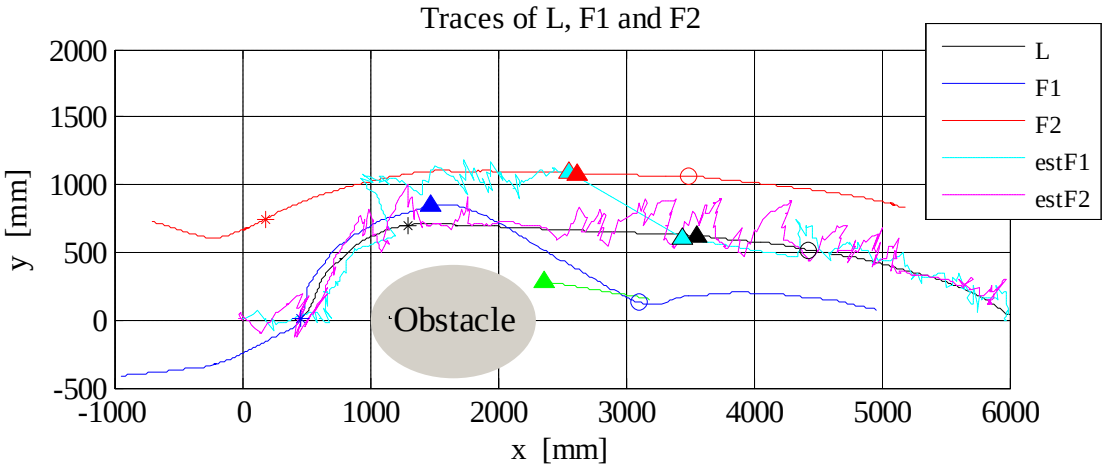

Figure 6: Traces of leader and followers and leader position estimated by followers; longitudinal-ellipsoidal obstacle.

Table 2: Mode flag numbers.

mode no.	mode
18	N-r-mode
19	N-s-mode
20	N-f-mode
21	Right in A-mode
22	Front in A-mode
23	Front-Right in A-mode
24	Left in A-mode
25	Left-Right in A-mode
26	Front-Left in A-mode
27	Left-Front-Right in A-mode
28	Back in A-mode
29	Wait in A-mode

IV. EXPERIMENTS OF FORMATION CONTROL

This section presents the results of formation control experiments using three real mobile robots; two Pioneer-1 and one Pioneer-3, to examine the proposed techniques, where three types of obstacle; longitudinal-ellipsoid, lateral-ellipsoid and wall, were examined. The original formation shape was given by *Triangle*, while the one for obstacle avoidance was *Line*. The relative distance and the relative angle were specified as follows.

* *Triangle* (shape No.=73)
F_1: d_{f1}^{rel} = 600 [mm], γ_{f1}^{rel} = 15 [deg]
F_2: d_{f2}^{rel} = 600 [mm], γ_{f2}^{rel} = -30 [deg]
* *Line* (shape No.=71)
F_1: d_{f1}^{rel} = 600 [mm], γ_{f1}^{rel} = 0 [deg]
F_2: d_{f2}^{rel} = 600 [mm], γ_{f2}^{rel} = 0 [deg]

The nominal linear velocity and the maximum command inputs were given as follows.
v_0=100 [mm/s], v_{max}=200 [mm/s], ω_{max}=10 [deg/s]
The sampling time was given by T_s=0.1 [s].

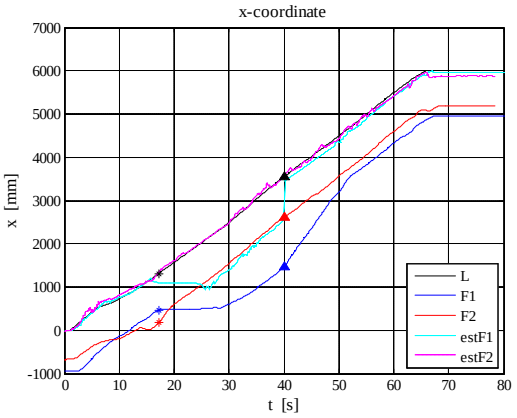

Figure 7: Time histories of x_l, x_{f1}, x_{f2} (solid-lines) and $\hat{x}_l$ estimated by F_1 and F_2 (dashed-lines); longitudinal-ellipsoidal obstacle.

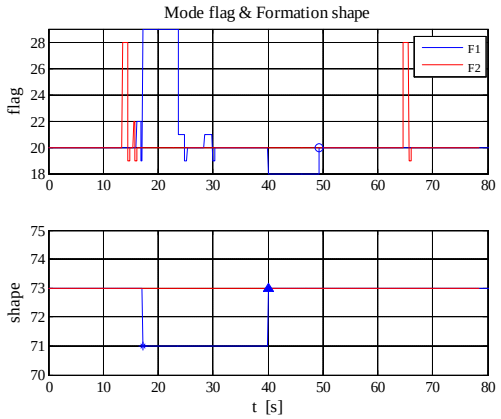

Figure 8: Time histories of mode flag and formation shape; longitudinal-ellipsoidal obstacle.

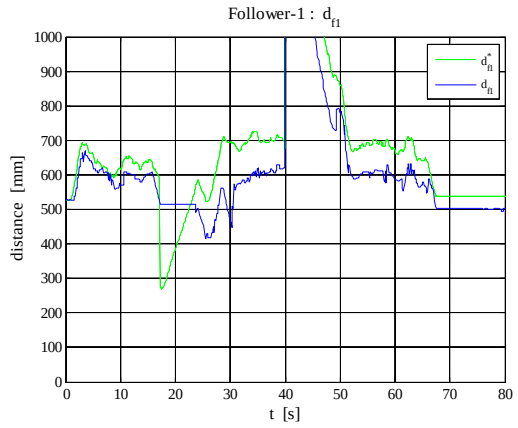

Figure 9: Time histories of relative distance d_{f1} and true relative distance d_{f1}^*; longitudinal-ellipsoidal obstacle.

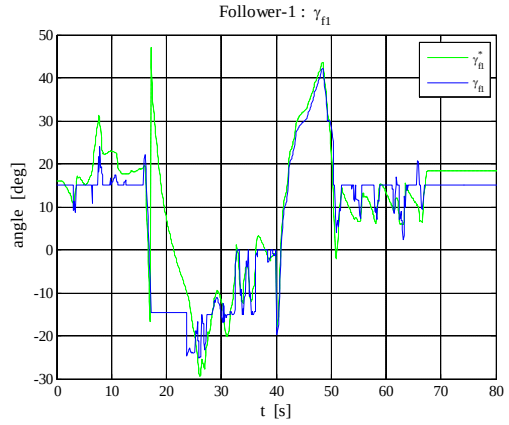

Figure 10: Time histories of relative angle γ_{f1} and true relative angle γ_{f1}^*; longitudinal-ellipsoidal obstacle.

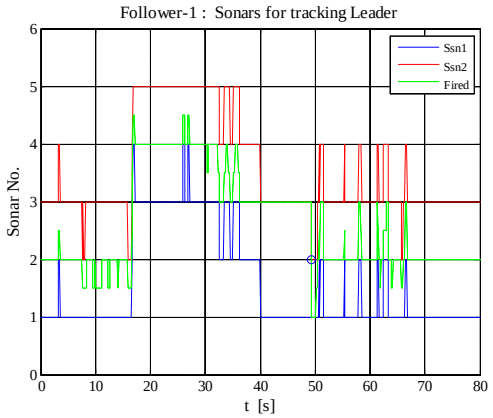

Figure 11: Time histories of upper and lower sonars for tracking leader robot; longitudinal-ellipsoidal obstacle.

A. Longitudinal-Ellipsoidal Obstacle

Figures 6 – 11 show the experimental results of the longitudinal-ellipsoidal obstacle case. In Figs. 6 and 7, the solid-lines show traces of L, F_1 and F_2 and the dashed-lines show traces of leader position estimated by F_1 and F_2. In this experiment, the start point of L was placed at the origin of the Cartesian coordinates (x,y), while the goal was located at (x_g,y_g)=(6000,0) [mm]. The positional coordinates of the robot were provided by the deadreckoning of each robot. Since the travel distance of the robots in the experiments of formation control was not so long, the accumulated error of the position was less than a few centimeters. As the experiment wanted to begin under the triangle formation, the three mobile robots were placed by making a triangle at start, where F_1 and F_2 were the right and the left back of L, respectively. An ellipsoidal obstacle whose size was approximately 1300 x 800 [mm] was longitudinally placed on the way between the start and the goal. The upper and the lower of Fig. 8 show the time histories of the mode flag and the formation shape of F_1 and F_2, respectively. The mode numbers are listed in Table 2.

After L avoided the obstacle, F_1 encountered the obstacle. According to the judge of *Form Change*, the formation shape of F_1 was changed to *Line* (shape No.=71) at t=17.2 [s] (see Fig. 8), and its leader robot was changed from L to F_2. The positions of L, F_1 and F_2 at this time are marked by the black, blue and red asterisks in Figs. 6 and 7, respectively. The leader position estimated by F_1, drawn by the cyan dashed-line, was shifted to the trace of F_2 as shown in Figs. 6 and 7. At t=40.0 [s], the relative distance from F_1 to the obstacle was longer than a threshold. Then, the mode of F_1 was changed to N-r-mode (flag No.=18), the reformation of F_1 began; that is, t_{kr}=40.0 [s]. The positions of L, F_1 and F_2 at this time are marked by the black, blue and red triangles in Figs. 6 and 7, respectively. After re-formation, the leader robot of F_1 was returned to L. Then using Eq. (14), the leader position estimated by F_1 was changed from the position marked by the red-edged cyan triangle (t_{kr-1}=39.9 [s]) to the one marked by the black-edged cyan triangle (t_{kr} =40.0 [s]) in Fig. 6. Comparing the cyan triangle to the red and the black triangles in Fig. 6, it is seen that the leader position was properly estimated. The target point P for re-constructing *Triangle* (shape No. = 73) was calculated by Eq. (8) at the position marked by the green triangle. F_1 then moved the target point with the maximum transitional velocity. The target point was also updated by Eq. (12) toward the goal with the nominal linear velocity. The reformation was finished at t=49.4 [s]. The positions of L, F_1 and F_2 at this time are marked by the black, blue and red circles in Fig. 6, respectively. The formation control by *Triangle* was re-constructed since F_1 detected L again after that.

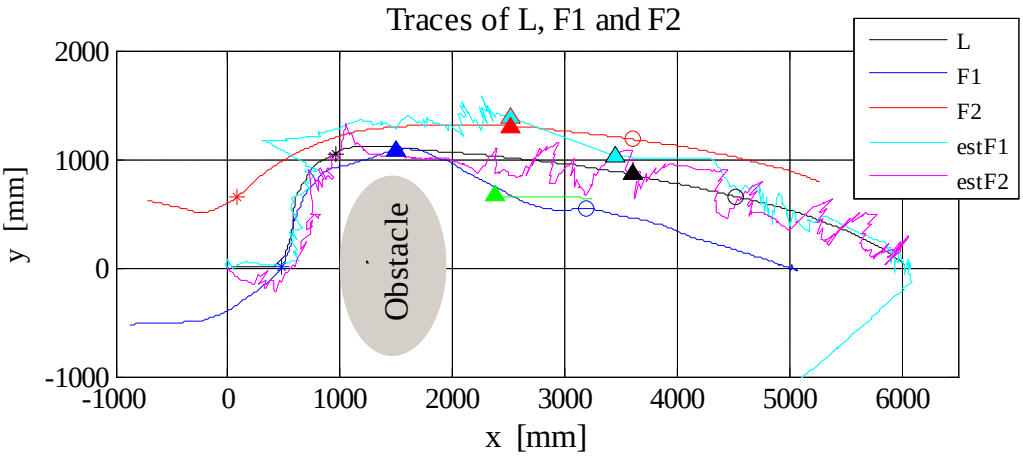

Figure 12: Traces of leader and followers and leader position estimated by followers; lateral-ellipsoidal obstacle.

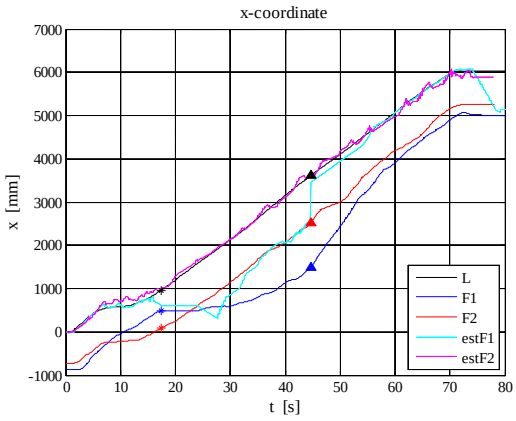

Figure 13: Time histories of x_l, x_{f1}, x_{f2} (solid-lines) and $\hat{x}_l$ estimated by F_1 and F_2 (dashed-lines); lateral-ellipsoidal obstacle.

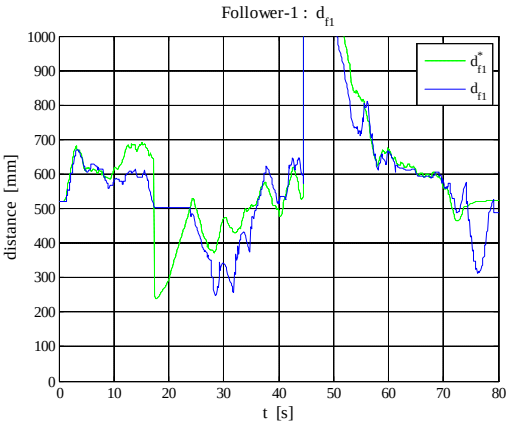

Figure 15: Time histories of relative distance d_{f1} and true relative distance d_{f1}^*; lateral-ellipsoidal obstacle.

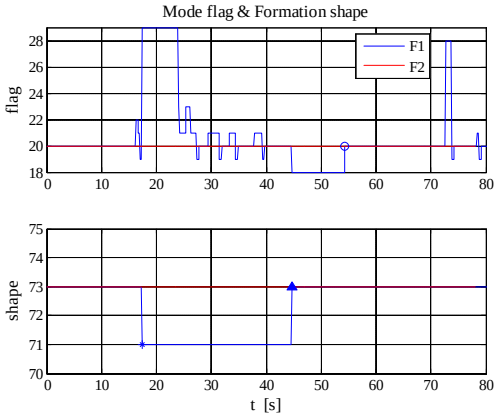

Figure 14: Time histories of mode flag and formation shape; lateral-ellipsoidal obstacle.

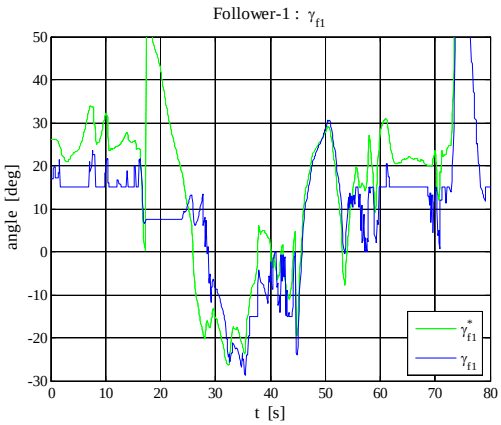

Figure 16: Time histories of relative angle γ_{f1} and true relative angle γ_{f1}^*; lateral-ellipsoidal obstacle.

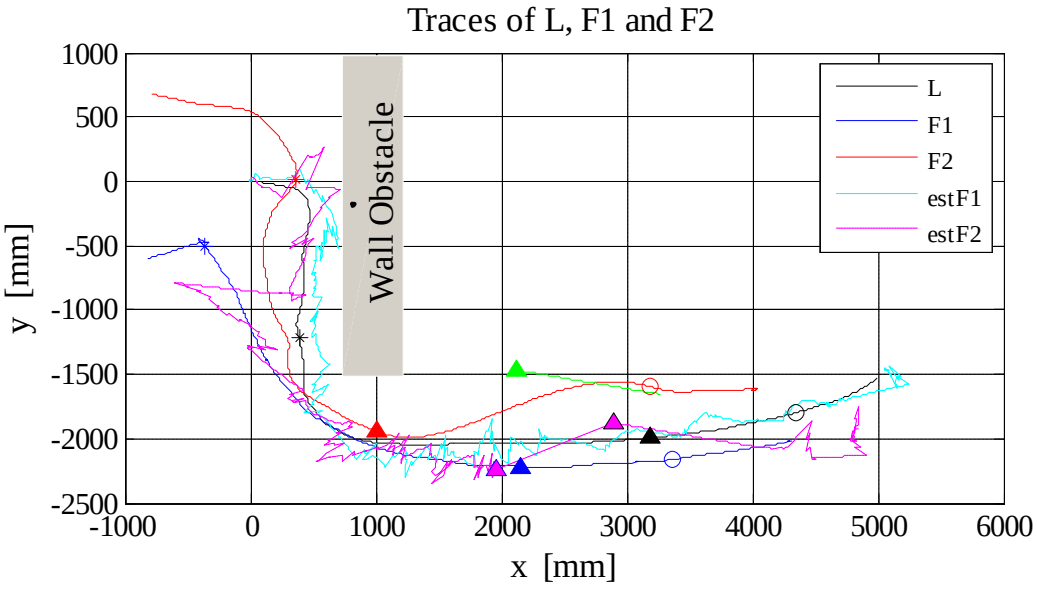

Figure 17: Traces of leader and followers and leader position estimated by followers; wall obstacle.

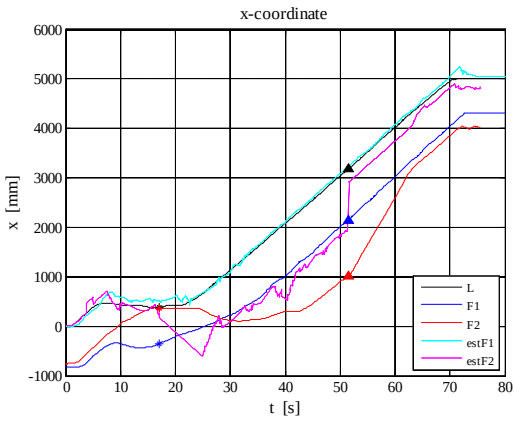

Figure 18: Time histories of x_l, x_{f1}, x_{f2} (solid-lines) and $\hat{x}_l$ estimated by F_1 and F_2 (dashed-lines); wall obstacle.

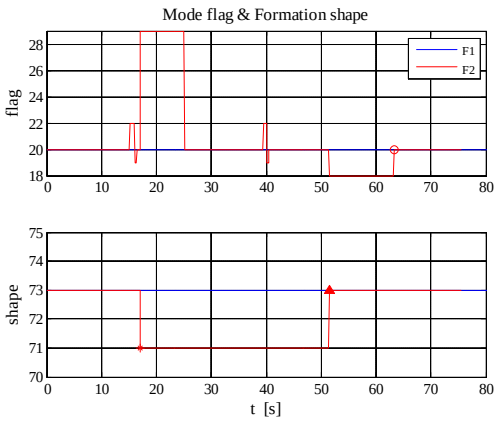

Figure 19: Time histories of mode flag and formation shape; wall obstacle.

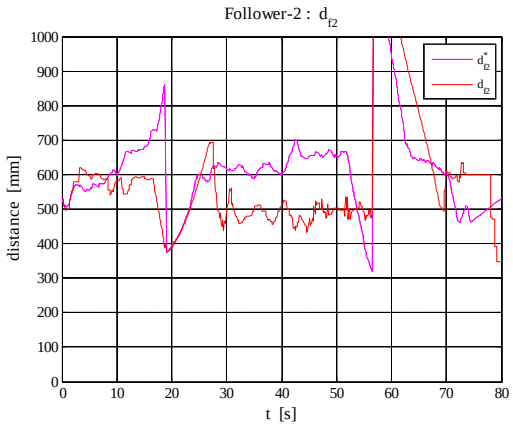

Figure 20: Time histories of relative distance d_{f2} and true relative distance d_{f2}^*; wall obstacle.

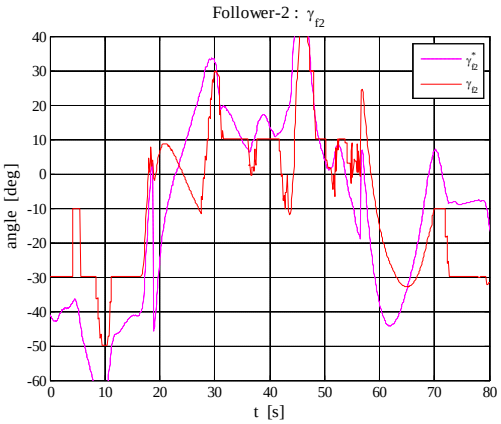

Figure 21: Time histories of relative angle γ_{f2} and true relative angle γ_{f2}^*; wall obstacle.

B. Lateral-Ellipsoidal Obstacle

The experimental results of the lateral-ellipsoidal obstacle case are shown in Fig. 12 – 16, where the ellipsoidal obstacle used in Section 4.1 was laterally placed. Compared to the results of the longitudinal-ellipsoidal obstacle case, the amount of avoidance of L and F_1 was increased. The time length which the formation shape was *Line* was approximately longer than five seconds. It is seen from these figures that formation control with the obstacle avoidance was succeeded.

C. Wall Obstacle

The experimental results of the wall obstacle case are shown in Fig. 17 – 21, where wall obstacle was laterally placed between the start and the goal. The goal of L was located at (x_g,y_g)=(5000,-1500) [mm]. This experiment examined the behaviors of F_2 with respect to the formation construction and obstacle avoidance.

Since the wall following was needed for avoiding the wall obstacle, the amount of avoidance was more increased and the time length during *Line* was extended (see lower in Fig. 19). Compared to the lateral-ellipsoidal obstacle case, F_1 at the change of formation shape was about just right-hand side of F_2 (check in Figs. 17 – 19 at t=17.1 [s]). For this positional situation, F_2 judged that the obstacle encountered was a wall. Then, a turning control was added at *Wait*; that is, the direction of F_2 was controlled toward F_1 during *Wait*. As the result, F_2 detected F_1 after *Wait* and began to follow F_1. When F_2 passed the lower border of the wall obstacle, F_2 behaved to avoid the wall a bit but did not fail to detect F_1 after that. F_2 finally accomplished to return the position of the original formation shape *Triangle*.

V. CONCLUSION

This paper has presented a formation control of multi-sonar equipped mobile robots with large obstacle avoidance. Based on the technique presented in [9], new strategies for avoiding large obstacle; that is, change of formation shape and re-formation and reinforce modules; that is, *Sonar Prediction* and *Move Prediction*, were newly introduced. Some modifications for improving drawbacks in [10] were also included in the proposed navigation algorithm. The effectiveness of the proposed techniques was demonstrated in the experiments using three real mobile robots with three types of obstacles; longitudinal-ellipsoid, lateral-ellipsoid and wall obstacles. The proposed navigation algorithm could be installed with a little parameter adjustment but without any serious problems in both Pioneer-1 and Pioneer-3 although number of multiple sonars was different. It means that the proposed techniques are useful for multi-sonar equipped mobile robots and are furthermore applicable in multi-obstacle scattered environments.

REFERENCES

[1] J.P. Desai and J.P. Ostrowski, and V. Kumar, Modelling and control of formations of nonholonomic mobile robots, *IEEE Transactions on Robotics and Automation*, 17*(6)*, 2001, 905-908.

[2] J.B. Park B.S. Park, and Y.H. Choi, Adaptive formation control of electrically driven nonholonomic mobile robots with limited information, *IEEE Transactions on Systems, Man and Cybernetics, Part B*, 41*(4)*, 2011, 1061-1075.

[3] T. Balch and R.C. Arkin. Behaviour-based formation control for multirobotic teams, *IEEE Transactions on Robotics and Automation*, 14*(6)*, 1998, 926-934.

[4] A. Rizzi R. Burridge and D. Koditschek. Sequential composition of dynamically dexterous robot behaviour, *The International Journal Robotics Research*, 18, 1999, 926-934.

[5] K.-H. Tan and A.M. Lewis, Virtual structures for high precision cooperative mobile robot control, *In IEEE/RSJ International Conference on Intelligent Robots and Systems*, 3, 1996, 132-139.

[6] A. Fujimori, T. Fujimoto, and G. Bohács, Formated navigation of mobile robots using distributed leader-follower control, *In 16th IFAC World Congress*, Prague, Czech Republic, July 2005.

[7] A. Fujimori, T. Saito, and G. Bohács, Formated navigation of mobile robots with obstacle avoidance, *In IEEE Conference on Robotics, Automation and Mechatronics*. Bangkok, Thailand, June 2006.

[8] A. Fujimori, T. Fujimoto, and G. Bohács, Mobile robot formation control using a modified leader-follower technique, *Integrated Computer-Aided Engineering*, 15*(1)*, 2008, 71-84.

[9] A. Fujimori, H. Kubota, N. Shibata, and Y. Tezuka, Leader follower formation control with obstacle avoidance using sonar-equipped mobile robots. *Journal of Systems and Control Engineering*, 228*(5)*, 2014, 303-315.

[10] A. Fujimori, A. Hosono, K. Takahashi, and S. Oh-hara, Formation control of multiple mobile robots with large obstacle avoidance, *In The 15th International Conference on Control, Automation, Robotics and Vision*, November, 2018.

[11] H.G. Tanner, G.J. Pappas, and V. Kumar. Leader-to-formation stability, *IEEE*

Transactions on Robotics and Automation, 20*(3)*, 2004, 443-455.
[12] ActivMedia Inc., *Pioneer 1 Operations Manual*, 1996.
[13] ActivMedia Inc., *Pioneer 1 Software Manual*, Version 4.1.2, 1996.
[14] ActivMedia Inc., *Pioneer 3 Operations Manual*, Version 2, 2015.

Atsushi Fujimori, et. al. "Formation Control of Multi-Sonar Equipped Mobile Robots and Large Obstacle Avoidance." *International Journal of Engineering Research and Applications (IJERA)*, vol.10 (07), 2020, pp 48-59.